Available online at www.sciencedirect.com
ScienceDirect
Journal of the European Ceramic Society 28 (2008) 3107–3112
www.elsevier.com/locate/jeurceramsoc

# Synthesis of nano-crystalline $Ce_{0.9}Gd_{0.1}O_{1.95}$ electrolyte by novel sol–gel thermolysis process for IT-SOFCs

D. Hari Prasad, J.-W. Son, B.-K. Kim, H.-W. Lee, J.-H. Lee *

*Center for Energy Materials Research, Korea Institute of Science and Technology, Seoul 136-791, Republic of Korea*

Received 9 March 2008; received in revised form 19 May 2008; accepted 19 May 2008
Available online 3 July 2008

**Abstract**

In the present work, nano-crystalline $Ce_{0.9}Gd_{0.1}O_{1.95}$ (GDC) powder has been successfully prepared by a novel sol–gel thermolysis method using a unique combination of urea and PVA. The gel precursor obtained during the process was calcined at 400 and 600 °C for 2 h. A range of analyzing techniques including XRD, TGA, BET, SEM, EDS and TEM were employed to characterize the physical and chemical properties of obtained powders. GDC gel precursors calcined at 400 and 600 °C were found to have an average crystallite size of 10 and 19 nm, respectively. From the result of XRD patterns, we found that well-crystalline cubic fluorite structure GDC was obtained by calcining the precursor gel at 400 and 600 °C. It has been also found that the sintered samples with lower temperature calcined powder showed better sinterability as well as higher ionic conductivity of $2.21 \times 10^{-2}$ S cm$^{-1}$ at 700 °C in air.


*Keywords:* Powders-chemical preparation; Microstructure-final; Ionic conductivity; $CeO_2$; Fuel cells

## 1. Introduction

Intermediate-temperature solid oxide fuel cells (IT-SOFCs) operating at 500–800 °C have attracted considerable interest in the recent years.[1] Lowering the operating temperature can minimize various problems associated with high temperature operation, such as ionic interdiffusions between electrode/electrolyte interfaces, coarsening of electrodes and chemical interaction in SOFC components. However lowered operating temperature inevitably induces the resistance increase of the electrolyte, which can be solved either by decreasing the electrolyte thickness or by introducing alternative materials with higher ionic conductivity at lower temperatures. With high ionic conductivity at relatively moderate temperature (above 600 °C), doped ceria has been extensively studied as electrolytes for SOFCs at intermediate temperatures.[1–4] Among various kind of doped ceria, gadolinium-doped ceria (GDC, $Ce_{0.9}Gd_{0.1}O_{1.95}$) is now considered to be one of the most promising electrolyte for IT-SOFCs to be operated below 800 °C as well as part of SOFC anodes which can be directly used for hydrocarbon fuels.[1,2]

Solid-state thermal reaction method has been generally employed to make GDC.[5,6] However it generally requires the long range diffusion of metal ions during the synthesis accompanied with prolonged calcination at high temperature. Furthermore it has many difficulties in controlling of stoichiometry as well as particle size. To overcome the above drawbacks various synthesis methods such as homogeneous precipitation,[7,8] sol–gels,[9] combustion using glycine as fuel,[10] using ammonia,[11] ammonium carbonate,[12,13] and hydrazine hydrate,[14] have been adopted for the synthesis of nano-crystalline materials. Among these, self-propagating combustion synthesis is mostly used for producing compositionally homogeneous and nano-crystalline powders. However this method holds some drawbacks to control the agglomeration of particles.[15] Hence there were some attempts to add some more polymers during combustion synthesis to reduce the agglomeration and thus provide well-dispersed nano-crystalline powders.[16,17] In this context, sol–gel thermolysis method can be introduced for the synthesis of nano-crystalline GDC powder. This sol–gel thermolysis process is a unique combination of a thermal process and a chemical gelation process. The organic polymer(s) not only act as an excellent fuel, but also control the particle size during the formation of gelation process and also prevent the aggregation of par-

* Corresponding author. Tel.: +82 29585532; fax: +82 29585529.
*E-mail address:* jongho@kist.re.kr (J.-H. Lee).

0955-2219/$ – see front matter © 2008 Elsevier Ltd. All rights reserved.
doi:10.1016/j.jeurceramsoc.2008.05.021

ticles during the thermolysis of the gel due to its long chain structure.[16,17]

In the present investigation, an attempt has been made for the first time to prepare well-dispersed nano-crystalline GDC powders by novel sol–gel thermolysis process using urea as the fuel for combustion process and polyvinyl alcohol (PVA) as the dispersing agent as well as secondary fuel. The effect of calcination temperature on the structural properties and morphology of the powders were studied by XRD, BET, SEM, and TEM analysis. Finally, sintering behavior and electrical conductivity of the calcined GDC powders have been investigated.

## 2. Experimental

### 2.1. Synthesis of GDC powder

The nano-crystalline GDC was synthesized by a novel sol–gel thermolysis process using urea (Yakuri Chemicals) as a combustion fuel and PVA (Aldrich Chemicals) as the dispersing agent as well as secondary fuel. In this method, stoichiometric amounts of $Ce(NO_3)_3{\cdot}6H_2O$ (Kanto Chemicals) and $Gd(NO_3)_3{\cdot}6H_2O$ (Aldrich Chemicals) were dissolved in distilled water and an aqueous solution of urea and PVA were added with constant stirring until a homogenous solution was achieved. As per the propellant chemistry, in combustion reaction the ratio of fuel to oxidant is fixed in such a way that the net reducing valency of the fuel equals to the net oxidizing valency of the oxidant.[16,18–20] The oxidizing valances of the oxidants and the reducing valency of fuel (urea) are given in Table 1.The molar ratio of fuel to metal nitrate has been determined based on the above concept. It may be mentioned here that the reducing valences of nitrogen and carbon have been taken as 0 and 4, respectively considering $N_2$ and $CO_2$ as the gaseous combustion products.

In this study, the equivalence ratio ($\emptyset_e$) was maintained to unity[21] and the amount of PVA was fixed just equal to the amount of urea taken. The prepared solution with aforementioned polymers was then heated to 80 °C to obtain viscous solution (sol) and continuously heated at same temperature until to obtain the gel state precursor sample. Finally, the obtained precursor sample was calcined at 400 and 600 °C for 2 h in air to obtain a single-phase GDC powders, which are designated hereafter as ST 400 and ST 600, respectively. The obtained powders were ground in an agate mortar and then pressed into pellets via cold isostatic pressing (CIP) under a pressure of 200 MPa. All the pellets were sintered at 1500 °C in air for 4 h for the characterization of microstructure and electrical properties.

Table 1
The oxidizing valences of oxidants and the reducing valences of urea

| Compound | Derivation | Valency oxidizing (−) reducing (+) |
|---|---|---|
| Oxidizers | | |
| $M(NO_3)_3$ M = Ce, Gd | $3+3x\{0+3(-2)\}$ | −15 |
| Fuel | | |
| Urea ($CH_4N_2O$) | $4+4x(1)+2x(0)+(-2)$ | +6 |

### 2.2. Characterization

The thermal decomposition behavior of the precursor sample was studied by thermo-gravimetric analysis (TA instrument, 2050 TGA V5.4A, USA) at the temperature range of 30–450 °C with a heating rate of 5 °C/min. The phase analysis was carried out via X-ray diffractometer (PW 3830 X-ray generator, Netherlands). The crystallite size was determined by means of Scherrer equation, $D = 0.9\lambda/\beta\cos\theta$, where $D$ is the crystallite size, $\lambda$ is the wavelength of the radiation, $\beta$ is the corrected peak width at half-maximum intensity and $\theta$ is the peak position. EDS/SEM (EDAX/SEM, XL-30 FEG ESEM, Netherlands) and TEM (Technai G2 F20, USA) were used for the compositional and microstructural analysis such as size, shape and morphology of the obtained powder and its agglomerates. The specific surface area of powders was measured by BET (Quantachrome Corporation Autosorb, USA). Particle size analyser (PSA) (Microtrac UPA 150, USA) was used to determine the average value of apparent particle size. The relative density of the sintered samples was estimated using the relation: relative density (%) = $(d_{th}/d_m) \times 100$, where $d_m$ is the density of the samples measured by Archimedes method and $d_{th}$ is the theoretical density of the GDC sample.

Thermal expansion measurements were conducted with a dilatometer (Netsch Dil 402C/3/G, Germany) in air, operated from 50 to 1500 °C (heating rate 3 °C $min^{-1}$, flow rate 50 ml $min^{-1}$). The conductivity of the specimen sintered at 1500 °C/4 h was measured in the temperature range of 500–900 °C in air by using the potentiostat/galvanostat (IVIUMSTAT, Netherlands) with four-point DC method. Before the measurement, Pt paste was painted onto both sides of the sintered pellets and fired at 1000 °C for 1 h to act as porous gas electrodes.

## 3. Results and discussion

Fig. 1 shows the TG curve for GDC precursor sample. The weight loss in the temperature of 30–130 °C corresponds to the

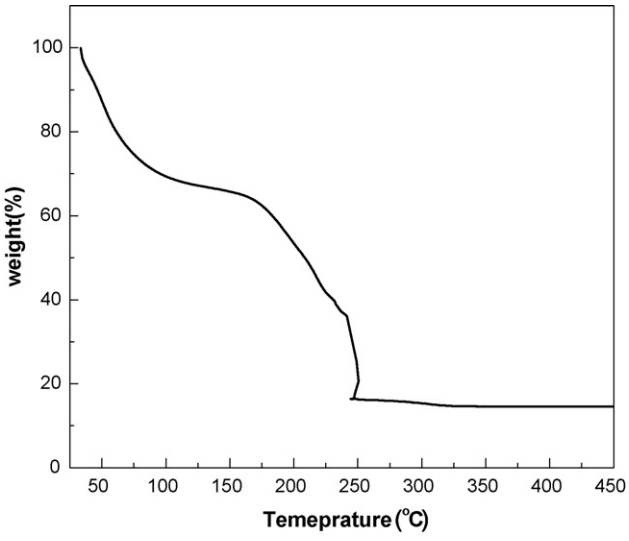


Fig. 1. TG analysis of GDC precursor sample.

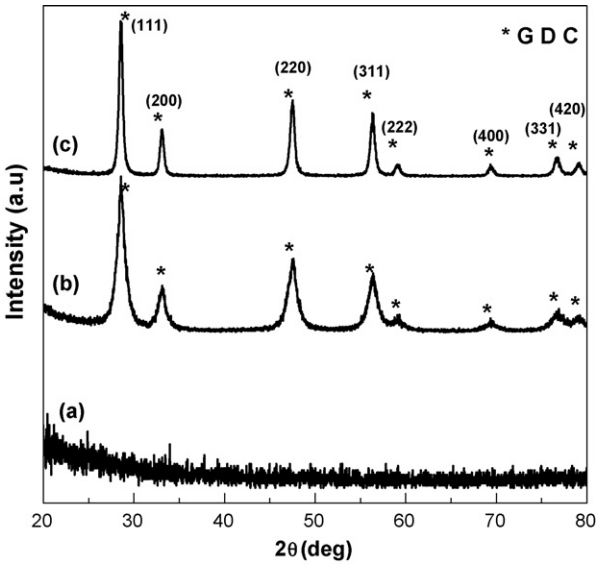


Fig. 2. XRD patterns of GDC. (a) Precursor gel, (b) ST 400, and (c) ST 600.

removal of the superficial and structural water in the gel precursor. The weight loss in the temperature range of 130–370 °C corresponds to the combustion of inorganic and organic constituents of the precursor, such as nitrates, urea, PVA.[16] Almost no loss was observed above 370 °C, implying only the presence of crystalline GDC. It was further confirmed by XRD measurements.

Fig. 2 illustrates the XRD patterns of the GDC samples. Fig. 2(a) shows the XRD peak of the precursor gel and Fig. 2(b) and (c) depicts those of ST 400 and ST 600 powders, respectively. ST 400 and ST 600 powders shows all main reflections of a typical cubic fluorite structure of GDC corresponding to (1 1 1), (2 0 0), (2 2 0), (3 1 1), (2 2 2), and (4 0 0) planes (JCPDS No. 75-0161). As can be seen at Fig. 2, as the calcination temperature increases the intensity of the peak becomes sharp and crystallinity of the powder increases. The calculated results of crystallite size from XRD and average value of apparent particle size from PSA are shown in Table 2.

As shown in Table 2, the equivalent particle size from BET is much smaller than the measured apparent particle size, indicating the obtained GDC powder is the agglomerated form of nano-crystalline primary particle. In this agglomerated form of powder, the primary particles are bonded together by forming necks at the active contact points. In this study, comparatively less degree of agglomeration was observed for ST 400 sample.

Table 2
Crystallite size, particle size, and surface area of sol–gel thermolysis synthesized GDC powders

| | ST 400 | ST 600 |
|---|---|---|
| Crystallite size (nm) from XRD | 10 | 19 |
| Apparent particle size (nm) from PSA | 1138 | 1893 |
| Surface area ($m^2$/g) from BET | 64 | 20 |
| Surface area equivalent particle size (nm) | 13 | 41 |
| Particle size from TEM | 11 | 21 |

Table 3
Compositional analysis of the GDC powder by using EDS analysis

| GDC powder | Element | wt% | mol% |
|---|---|---|---|
| ST 400 | Ce | 89.27 | 90.33 |
| | Gd | 10.72 | 9.67 |
| ST 600 | Ce | 87.93 | 89.12 |
| | Gd | 12.06 | 10.88 |

GDC composition of ST 400 and ST 600 was confirmed from EDS analysis which is shown in Table 3.

SEM images of ST 400 and ST 600 samples are shown in Fig. 3. As shown in Fig. 3(a) and (b), the particles are agglomerated and its size is increased with the increase in calcination temperature. Fig. 4 shows the TEM images of the calcined samples which showed the averages particle sizes were around 10–11

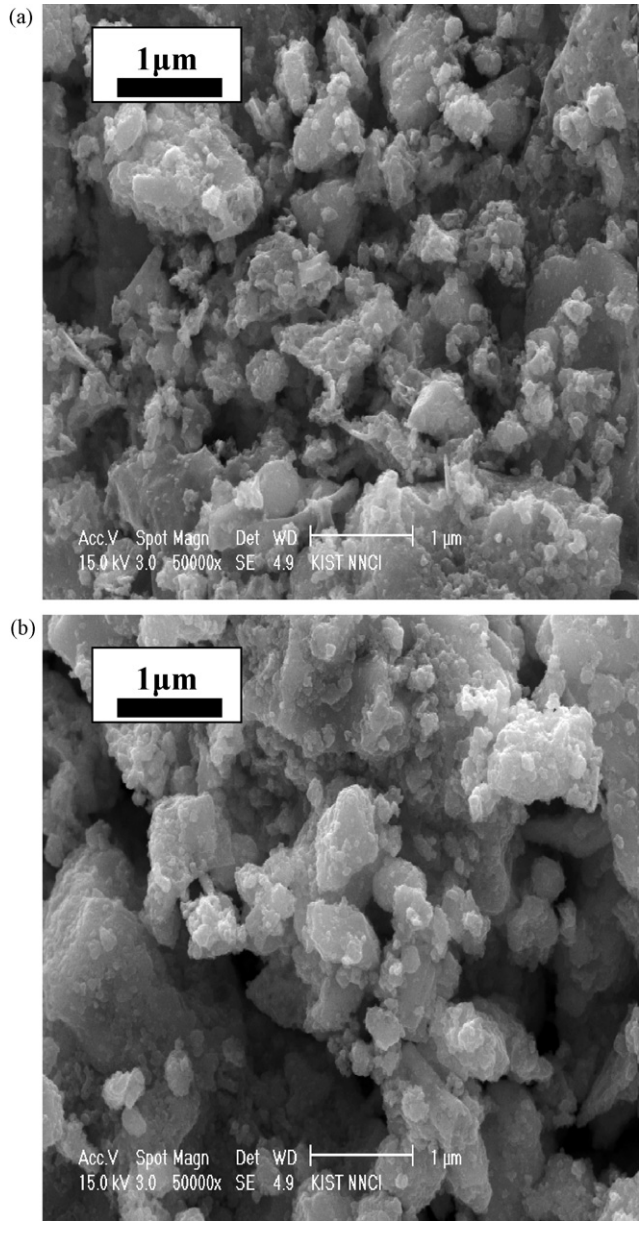


Fig. 3. SEM images of GDC. (a) ST 400 and (b) ST 600.

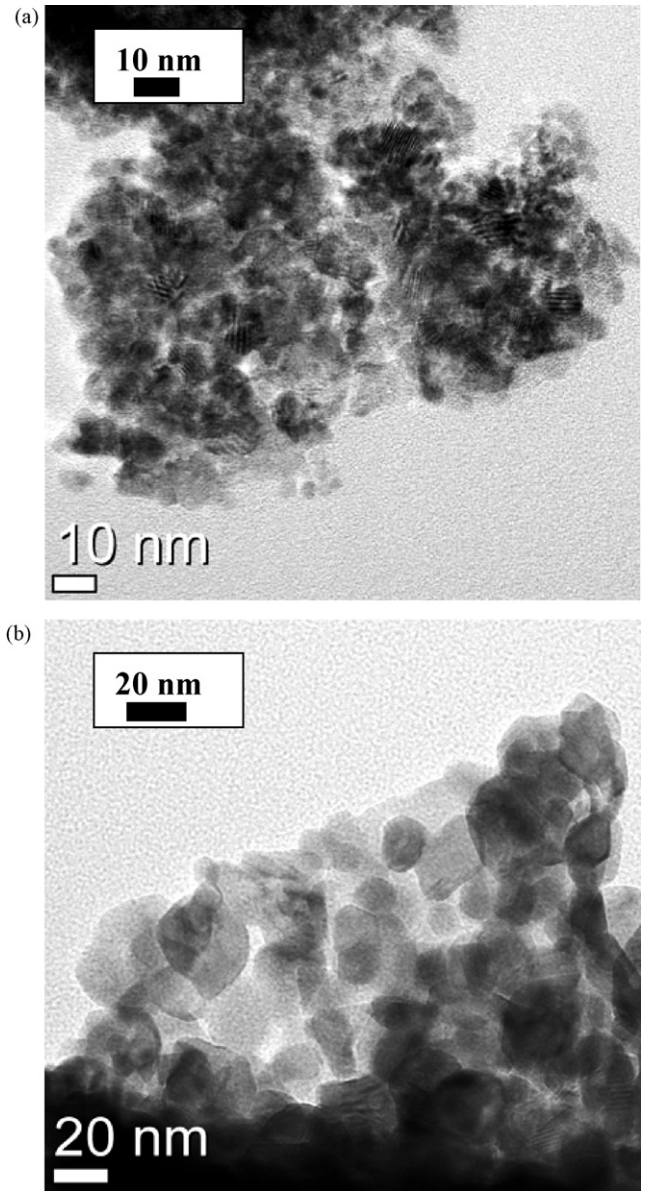


Fig. 4. TEM images of GDC. (a) ST 400 and (b) ST 600.

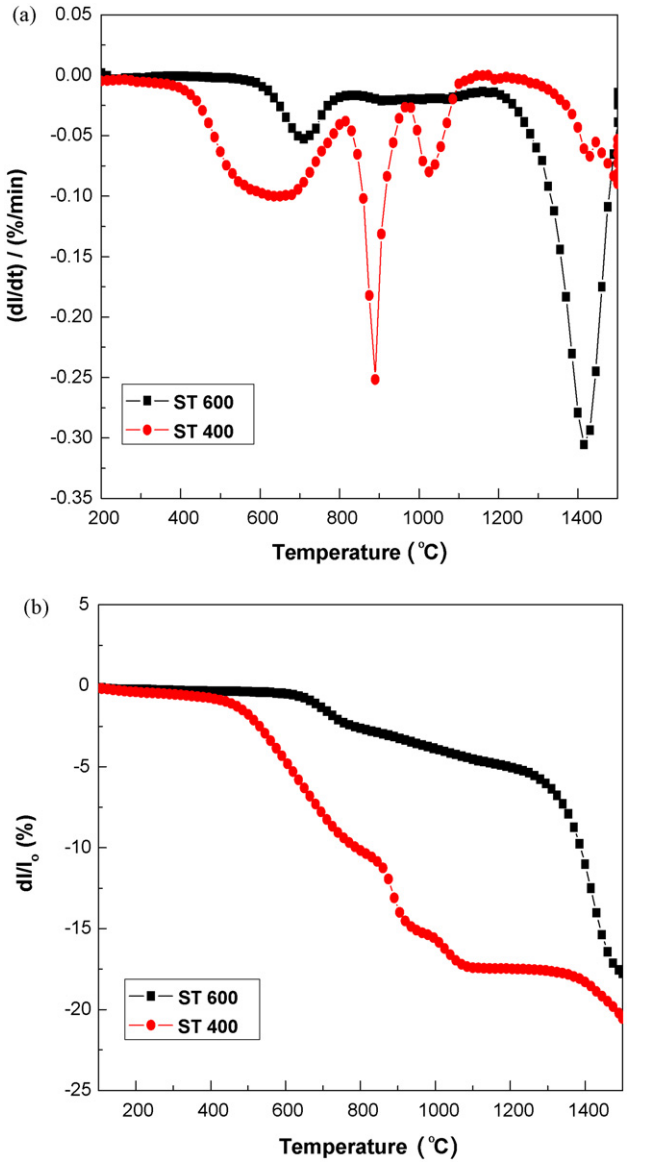


Fig. 5. Sintering behavior of ST 400 and ST 600. (a) Shrinkage rate spectra and (b) linear shrinkage.

and 19–21 nm for ST 400 (Fig. 4(a)) and ST 600 (Fig. 4(b)) samples, respectively. As shown in Fig. 4, the average particle sizes from TEM image are almost same to the crystallite sizes calculated by using Scherer equation from XRD.

Dilatometric measurements up to 1500 °C were made to study the sintering behavior of ST 400 and ST 600 samples. The Shrinkage rate spectra and linear shrinkage of the ST 400 and ST 600 are shown in Fig. 5(a) and (b), respectively. From the Fig. 5(a), the sintering process of ST 600 sample takes place with appearance of two shrinkage maxima, a small one at about 700 °C and the second one with higher shrinkage rate at about 1400 °C and the sintering process of ST 400 sample showed multi-step shrinkage behavior with shrinkage maxima at 500, 900 and 1050 °C. The great difference in shrinkage behavior between ST 400 and ST 600 is mainly coming from the different compaction behavior of two powders with different agglomerate strength. Relatively hard agglomerate in ST 600 powder kept its original shape during compaction, which remained relatively larger and uniform sized pores in between the hard agglomerate even after the compaction. Meanwhile relatively soft agglomerate in ST 400 could be easily broken which can eliminate larger inter-granular pores and produce relatively smaller pores with various size distributions. Hence ST 400 sample showed multiple shrinkage behavior at relatively lower temperature with multiple steps while ST 600 showed simple shrinkage behavior at relatively higher temperature.

Fig. 5(b) shows the linear shrinkage of ST 400 and ST 600 samples. As shown in Fig. 5(b) ST 600 sample did not reached to full shrinkage below 1500 °C with shrinkage of about 18%, while ST 400 sample reached nearly 18% shrinkage at relatively lower temperature of 1100 °C even though some slight additional shrinkage due to hard agglomerates were observed at around 1400–1450 °C.

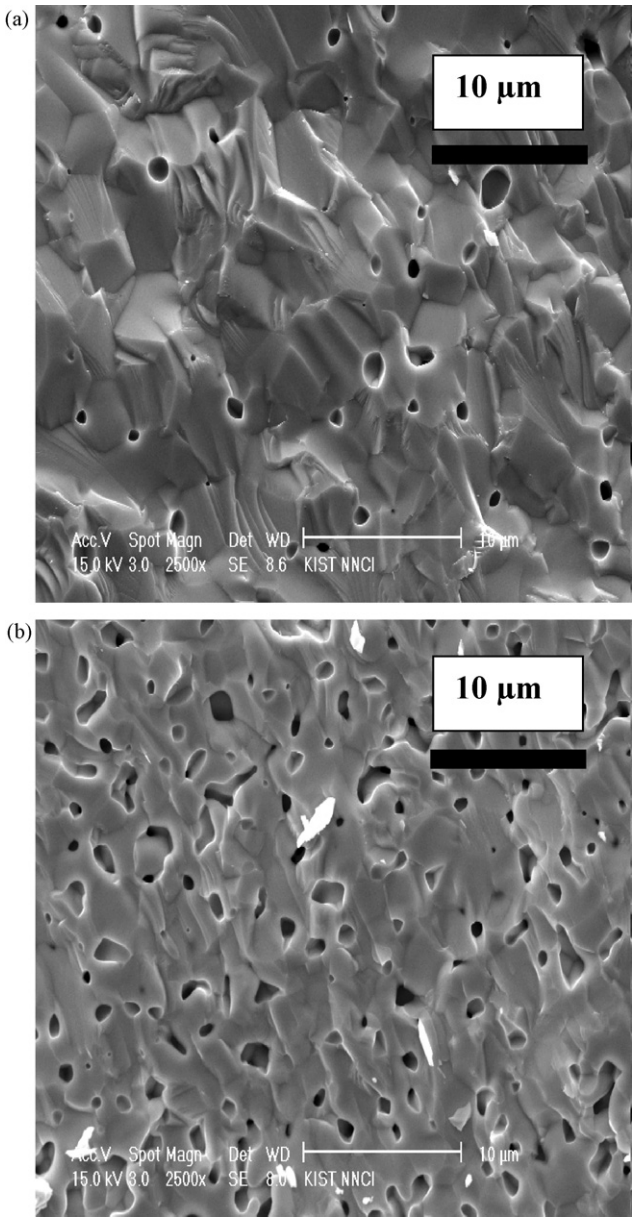


Fig. 6. Microstructure of GDC samples sintered at 1500 °C for 4 h in air. (a) ST 400 and (b) ST 600.

In this study, ST 400 and ST 600 samples were sintered at 1500 °C for 4 h in air to observe the microstructural effects on electrical conductivity. From the Archimedes method, the relative densities of the sintered samples for ST 400 and ST 600 samples were obtained as 96% and 92%, respectively. Fig. 6 shows SEM micrographs of ST 400 and ST 600 samples sintered at 1500 °C for 4 h. As shown in Fig. 6, a dense microstructure was observed for ST 400 sample whereas many pores still existed in ST 600 sample in accordance with the measured density from Archimedes method.

Fig. 7 presents an Arrhenius plot for the sintered ST 400 and ST 600 samples. It is well known that doped ceria behave as pure ionic conductor in air with negligible electronic conductivity. From the data presented in Fig. 7, the GDC conductivities reported in this work are similar to those reported in the

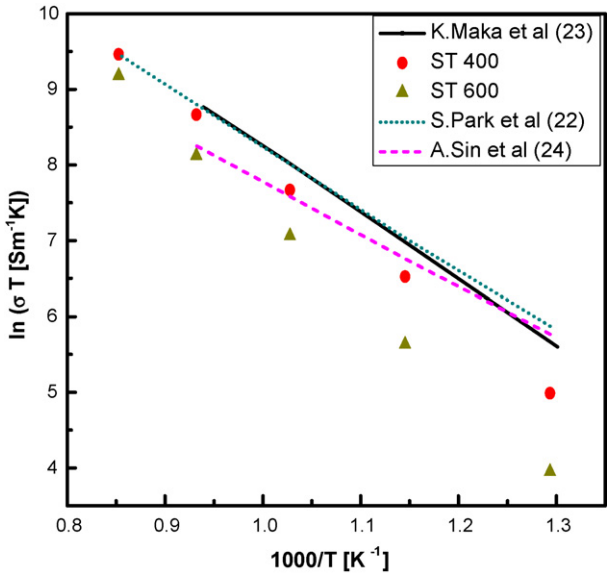


Fig. 7. Arrhenius plot of ionic conductivity of sintered GDC samples prepared by sol–gel thermolysis process.

literature.[22–24] Furthermore the activation energy ($E_a$ = 0.87 eV) was smaller in ST 400 sample than ST 600 sample, all of these differences in conductivity and activation energy, can be explained by the difference in relative density. The increase of ionic conductivity of GDC ceramics with increasing density of samples was also observed by Torrens et al. (relative density range 86–98%)[25] and by Ivanov et al. (relative density range 94–100%).[26] Similar to our results, these authors also mentioned a slight increase in $E_a$ with decrease in relative density.

## 4. Conclusions

Nano-crystalline GDC powder has been prepared successfully by a novel sol–gel thermolysis method. After calcination at 400 and 600 °C, all the synthesized GDC powders showed cubic fluorite structure with good crystallinity. From the particle size analysis with XRD, BET and PSA, we found that ST 600 powder is a little bit more agglomerated than ST 400 and has larger crystallite size, which has been confirmed from the SEM and TEM analysis. Such different characteristics in particle size and agglomeration induced different sintering behaviors that ST 400 showed better sinterability resulted in getting higher relative density than ST 600. As a consequence ST 400 sample showed higher electrical conductivity, which can be, used as an electrolyte material for IT-SOFCs.

## Acknowledgements

This work was supported by the Institutional Research Program and NRL Program of Korea Institute of Science and Technology.

## References

1. Steele, B. C. H., Appraisal of $Ce_{1-y}Gd_yO_{2-y/2}$ electrolytes for IT-SOFC operation at 500 °C. *Solid State Ionics*, 2000, **129**, 95–110.

2. Singhal, S. C., Advances in solid oxide fuel cell technology. *Solid State Ionics*, 2000, **135**, 305–313.
3. Mogensen, M., Sammesm, N. M. and Tompett, G. A., Physical, chemical and electrochemical properties of pure and doped ceria. *Solid State Ionics*, 2000, **129**, 63–94.
4. Sahibzada, M., Steele, B. C. H., Hellgardt, K., Barth, D., Effendi, A., Mantzavinos, D. and Metcalfe, I. S., Intermediate temperature solid oxide fuel cells operated with methanol fuels. *Chem. Eng. Sci.*, 2000, **55**, 3077–3083.
5. Chourashiya, M. G., Patil, J. Y., Pawar, S. H. and Jadhav, L. D., Studies on structural, morphological and electrical properties of $Ce_{1-x}Gd_xO_{2-(x/2)}$. *Mater. Chem. Phys.*, 2008, **109**, 39–44.
6. Kudo, T. and Obayashi, H., Oxygen ion conduction of the fluorite-type $Ce_{1-x}Ln_xO_{2-x/2}$. *J. Electrochem. Soc.*, 1975, **122**, 142–147.
7. Van Herle, J., Horita, T., Kawada, T., Sakai, N., Yokakawa, H. and Dokiya, M., Fabrication and sintering of fine yttria-doped ceria powder. *J. Am. Ceram. Soc.*, 1997, **80**(4), 933–940.
8. Zha, S. W., Fu, Q. X., Lang, Y., Xia, C. R. and Meng, G., Novel azeotropic distillation process for synthesizing nanoscale powders of yttria doped ceria electrolyte. *Mater. Lett.*, 2001, **47**, 351–355.
9. Huang, W., Shuk, P. and Greenblatt, M., Properties of sol–gel prepared $Ce_{1-x}Sm_xO_{2-x/2}$ solid electrolytes. *Solid State Ionics*, 1997, **100**, 23–27.
10. Xia, C. R., Chen, F. L. and Liu, M. L., Reduced-temperature solid oxide fuel cells fabricated by screen printing. *Electrochem. Solid State Lett.*, 2001, **4**(5), A52–A54.
11. Chiang, Y. M., Lavik, E. B. and Blom, D. A., Defect thermodynamics and electrical properties of nanocrystalline oxides: pure and doped $CeO_2$. *Nanostruct. Mater.*, 1997, **9**, 633–642.
12. Li, J. L., Ikegami, T. and Mori, T., Low temperature of dense samarium-doped $CeO_2$ ceramics: sintering and grain growth behaviors. *Acta Mater.*, 2004, **52**(8), 2221–2228.
13. Tok, A. I. Y., Luo, L. H. and Boye, F. Y. C., Carbonate Co-precipitation of $Gd_2O_3$-doped $CeO_2$ solid solution nano-particles. *Mater. Sci. Eng. A*, 2004, **383**, 229–234.
14. Kirk, T. J. and Winnick, J., A hydrogen sulfide solid-oxide fuel cell using ceria-based electrolytes. *J. Electrochem. Soc.*, 1993, **140**(12), 3494–3496.
15. Dan, L., Zhongyang, L., Yu, C. and Kefa, C., Study on agglomeration and densification behaviors of gadolinium-doped ceria ceramics. *J. Rare Earths*, 2007, **25**, 163–167.
16. Subramania, A., Sarada, T. and Muzhumathi, S., Synthesis of nanocrystalline $(Ba_{0.5}Sr_{0.5})$ $Co_{0.8}Fe_{0.2}O_{3-\delta}$ cathode material by a novel sol–gel thermolysis process for IT-SOFCs. *J. Power Sources*, 2007, **165**, 728–732.
17. Subramania, A., Angayarkanni, N. and Vasudevan, T., Effect of PVA with various combustion fuels in sol–gel thermolysis process for the synthesis of $LiMn_2O_4$ nanoparticles for Li-ion batteries. *Mater. Chem. Phys.*, 2007, **102**, 19–23.
18. Jain, S. R., Adiga, K. C. and Vernekar, V. R. P., A new approach to thermo chemical calculations of condensed fuel-oxidizer mixtures. *Combust. Flame*, 1981, **40**, 71–79.
19. Fu, Y. P., Microwave-induced combustion synthesis and ionic conductivity of $Ce_{0.8}(Gd_{0.2-x}Sm_0)O_{1.90}$. *Ceram. Int.*, doi:10.1016/j.ceramint.2007.07.026.
20. Gopi Chandran, R., Patil, K. C. and Chandrappa, G. T., Combustion synthesis, characterization of mullite-cordierite composites. *J. Mater. Sci. Lett.*, 1995, **14**, 548–551.
21. Park, H. R., Han, Y. S., Kim, D. K. and Kim, C. H., Synthesis of $LaCrO_3$ powders by microwave induced combustion of metal–urea mixture solution. *J. Mater. Sci. Lett.*, 1998, **17**, 785–787.
22. Park, S.-H. and Yoo, H.-I., Defect-chemical role of Mn in Gd-doped $CeO_2$. *Solid State Ionics*, 2005, **176**, 1485–1490.
23. Maka, K., Cihlar, J., Castkova, K., Zmeskal, O. and Hadraba, H., Sintering of gadolinia-doped ceria prepared by mechanochemical synthesis. *J. Eur. Ceram. Soc.*, 2007, **27**, 4345–4348.
24. Sin, A., Yu, D., Zaopo, A., Arico, A. S., Gullo, L., La Rosa, D., Siracusano, S., Antonucci, V., Oliva, C. and Ballabio, O., Preparation and sintering of $Ce_{1-x}Gd_xO_{2-x/2}$ nano-powders and their electrochemical and EPR characterization. *Solid State Ionics*, 2004, **175**, 361–366.
25. Torrens, R. S., Sammes, N. and Tompsett, M., Characterization of $(CeO_2)_{0.8}(GdO_{1.5})_{0.2}$ synthesized using various techniques. *Solid State Ionics*, 1998, **111**, 9–15.
26. Ivanov, V. V., Khrustov, V. R., Kotov, Y. A., Medvedev, A. I., Murzakaev, A. M., Shkerin, S. N. and Nikonov, A. V., Conductivity and structure features of $Ce_{1-x}Gd_xO_{2-\delta}$ solid electrolytes fabricated by compaction and sintering of weekly agglomerated nanopowders. *J. Eur. Ceram. Soc.*, 2007, **27**, 1041–1046.